

# Tryptophan 207 is crucial to the unique properties of the human voltage-gated proton channel, hH<sub>V</sub>1

Vladimir V. Cherny,<sup>1</sup> Deri Morgan,<sup>1</sup> Boris Musset,<sup>2</sup> Gustavo Chaves<sup>2</sup>, Susan M.E. Smith,<sup>3</sup> and Thomas E. DeCoursey<sup>1</sup>

<sup>1</sup>Department of Molecular Biophysics and Physiology, Rush University, Chicago, IL 60612

<sup>2</sup>Institute of Complex Systems 4 Zelluläre Biophysik, Forschungszentrum Jülich, 52425 Jülich, Germany

<sup>3</sup>Department of Molecular and Cellular Biology, Kennesaw State University, Kennesaw, GA 30144

Part of the “signature sequence” that defines the voltage-gated proton channel (H<sub>V</sub>1) is a tryptophan residue adjacent to the second Arg in the S4 transmembrane helix: RxWRxxR, which is perfectly conserved in all high confidence H<sub>V</sub>1 genes. Replacing Trp<sup>207</sup> in human H<sub>V</sub>1 (hH<sub>V</sub>1) with Ala, Ser, or Phe facilitated gating, accelerating channel opening by 100-fold, and closing by 30-fold. Mutant channels opened at more negative voltages than wild-type (WT) channels, indicating that in WT channels, Trp favors a closed state. The Arrhenius activation energy,  $E_a$ , for channel opening decreased to 22 kcal/mol from 30–38 kcal/mol for WT, confirming that Trp<sup>207</sup> establishes the major energy barrier between closed and open hH<sub>V</sub>1. Cation- $\pi$  interaction between Trp<sup>207</sup> and Arg<sup>211</sup> evidently latches the channel closed. Trp<sup>207</sup> mutants lost proton selectivity at p*H*<sub>o</sub> >8.0. Finally, gating that depends on the transmembrane pH gradient ( $\Delta$ pH-dependent gating), a universal feature of H<sub>V</sub>1 that is essential to its biological functions, was compromised. In the WT hH<sub>V</sub>1,  $\Delta$ pH-dependent gating is shown to saturate above p*H*<sub>i</sub> or p*H*<sub>o</sub> 8, consistent with a single pH sensor with alternating access to internal and external solutions. However, saturation occurred independently of  $\Delta$ pH, indicating the existence of distinct internal and external pH sensors. In Trp<sup>207</sup> mutants,  $\Delta$ pH-dependent gating saturated at lower p*H*<sub>o</sub> but not at lower p*H*<sub>i</sub>. That Trp<sup>207</sup> mutation selectively alters p*H*<sub>o</sub> sensing further supports the existence of distinct internal and external pH sensors. Analogous mutations in H<sub>V</sub>1 from the unicellular species *Karodinium veneficum* and *Emiliania huxleyi* produced generally similar consequences. Saturation of  $\Delta$ pH-dependent gating occurred at the same p*H*<sub>o</sub> and p*H*<sub>i</sub> in H<sub>V</sub>1 of all three species, suggesting that the same or similar group(s) is involved in pH sensing. Therefore, Trp enables four characteristic properties: slow channel opening, highly temperature-dependent gating kinetics, proton selectivity, and  $\Delta$ pH-dependent gating.

## INTRODUCTION

Voltage-gated proton channels (H<sub>V</sub>1) exist in diverse organisms ranging from unicellular marine species (Smith et al., 2011; Taylor et al., 2011) to humans (Ramsey et al., 2006). Their functions are equally diverse: conversion of CO<sub>2</sub> to calcite in coccolithophores (Taylor et al., 2011), triggering the bioluminescent flash in dinoflagellates (Smith et al., 2011), and in humans participating in innate immunity (DeCoursey, 2010), B cell signaling (Capasso et al., 2010), airway acid secretion (Iovannisci et al., 2010), histamine secretion (Musset et al., 2008b), sperm motility (Musset et al., 2012) and capacitation (Lishko et al., 2010), brain damage in ischemic stroke (Wu et al., 2012), breast cancer (Wang et al., 2012), and chronic lymphocytic leukemia (Hondares et al., 2014). All known and suspected H<sub>V</sub>1 to date, even in species with just 15–18% sequence identity to the human H<sub>V</sub>1 (hH<sub>V</sub>1), share a perfectly conserved tryptophan (Trp<sup>207</sup> in hH<sub>V</sub>1) adjacent to the second of three

Arg residues in the S4 transmembrane segment (Fig. S1) (DeCoursey, 2013). This Trp is part of the proposed signature sequence of the proton channel RxWRxxR (Smith et al., 2011), and is present even in several unconfirmed H<sub>V</sub>1-like sequences in fungi in which the third Arg in S4 is replaced by Lys (e.g., *Fusarium oxysporum*, *Ophiostoma piceae*, and *Metarhizium anisopliae*). Among molecules that contain voltage-sensing domains (VSDs), only H<sub>V</sub>1 and c15orf27 (whose function is unknown) contain Trp in this location (Smith et al., 2011). Here, we ask why this Trp has been conserved. We find that replacing Trp modifies four characteristic properties of hH<sub>V</sub>1, revealing that it is central to the unique defining properties and functions of H<sub>V</sub>1. Trp mutants opened and closed 30–100 times faster than WT, with gating kinetics less profoundly sensitive to temperature; they lost proton selectivity at high p*H*<sub>o</sub>; and the unique  $\Delta$ pH dependence of gating was compromised. The striking

Correspondence to Thomas E. DeCoursey: tdecours@rush.edu

Abbreviations used in this paper: CiVSP, *Ciona intestinalis* voltage-sensing phosphatase; hH<sub>V</sub>1, human voltage-gated proton channel; H<sub>V</sub>1, voltage-gated proton channel; VSD, voltage-sensing domain.

The Rockefeller University Press \$30.00  
J. Gen. Physiol. Vol. 146 No. 5 343–356  
www.jgp.org/cgi/doi/10.1085/jgp.201511456

© 2015 Cherny et al. This article is distributed under the terms of an Attribution–Noncommercial–Share Alike–No Mirror Sites license for the first six months after the publication date (see <http://www.rupress.org/terms>). After six months it is available under a Creative Commons License (Attribution–Noncommercial–Share Alike 3.0 Unported license, as described at <http://creativecommons.org/licenses/by-nc-sa/3.0/>).

Supplemental Material can be found at:  
<http://jgp.rupress.org/content/suppl/2015/10/06/jgp.201511456.DC1.html>

diversity of the effects of Trp mutation indicates that this residue plays a pivotal role in the H<sub>V1</sub> protein.

Tryptophan is the rarest amino acid in proteins, and in membrane proteins, it is often found close to lipid head groups, preferring the interfacial environment (Killian and von Heijne, 2000; MacCallum et al., 2008). Thus, the absolute conservation of a Trp in the middle of the S4 transmembrane segment of H<sub>V1</sub> requires some explanation. Three other Trp residues in hH<sub>V1</sub> are all in the intracellular N terminus. Perhaps because both Trp and Arg residues share ambivalence by exhibiting hydrophobic mixed with polar characteristics, they interact strongly with each other (Santiveri and Jiménez, 2010). In  $\beta$ -hairpin peptides and in other proteins, the guanidinium group of Arg stacks against the aromatic ring of Trp via cation- $\pi$  (Gallivan and Dougherty, 1999) and van der Waals interactions, stabilizing the protein structure (Tatko and Waters, 2003; Santiveri and Jiménez, 2010). The proximity of Trp<sup>203</sup> and R3 (the third Arg in the S4 segment, Arg<sup>207</sup> in mouse) in the closed structure of the mouse H<sub>V1</sub> (mH<sub>V1</sub>; Takeshita et al., 2014) appears to be consistent with this type of interaction, with amino-aromatic distances <6.0 Å (Burley and Petsko, 1986). In the structure identified as a closed conformation of mH<sub>V1</sub> (Takeshita et al., 2014), the indole side chain of Trp<sup>203</sup> is directed away from the pore toward the interior of the lipid bilayer, pointing downward, partially shielding the R3 side chain, which is directed down and between S4 and S3 but also has some lipid exposure. In all open-state models (Ramsey et al., 2010; Wood et al., 2012; Kulleperuma et al., 2013; Chamberlin et al., 2014), all three Arg residues of the S4 segment face the pore, but Trp still faces away from the pore. We propose that Trp stabilizes the closed hH<sub>V1</sub> through cation- $\pi$  interaction with Arg<sup>211</sup>, and that loss of this stabilization contributes to the consequences of its mutation. A striking result was that whether Trp was replaced by Ala (hydrophobic), Ser (hydrophilic), or Phe (aromatic), H<sub>V1</sub> properties were changed by a quantitatively indistinguishable extent. This result suggests that the heterocyclic aromatic side chain of Trp uniquely anchors the S4 segment in the membrane.

## MATERIALS AND METHODS

### Gene expression

Site-directed mutants were created using the QuikChange (Agilent Technologies) procedure according to the manufacturer's instructions. Transfection was done as described previously (Kulleperuma et al., 2013). Both HEK-293 cells and COS-7 cells were used as expression systems. We showed previously that the properties of H<sub>V1</sub> expressed in both cell lines were indistinguishable (Musset et al., 2008a). No other voltage- or time-dependent conductances were observed under the conditions of this study. Although most mutations on hH<sub>V1</sub> were introduced into a Zn<sup>2+</sup>-insensitive background (H140A/H193A), which we have done previously as a

control for endogenous H<sub>V1</sub> (Musset et al., 2011), the level of expression of all mutants studied here was sufficiently high that contamination by native H<sub>V1</sub> was negligible.

### Electrophysiology

In most experiments, cells expressing green fluorescent protein (GFP)-tagged proton channels were identified using inverted microscopes (Nikon) with fluorescence capability. For constructs that lacked the GFP tag, GFP was cotransfected. Conventional patch-clamp techniques were used (Kulleperuma et al., 2013) at room temperature (20–26°C). Bath and pipette solutions contained 60–100 mM buffer, 1–2 mM CaCl<sub>2</sub> or MgCl<sub>2</sub> (intracellular solutions were Ca<sup>2+</sup> free), 1–2 mM EGTA, and TMAMeSO<sub>3</sub> to adjust the osmolality to ~300 mOsm, titrated with TMAOH. Buffers used were Homo-PIPES (Research Organics) at pH 4.5–5.0, Mes at pH 5.5–6.0, BisTris at pH 6.5, PIPES at pH 7.0, HEPES at pH 7.5, tricine at pH 8.0, CHES at pH 9.0, and CAPS at pH 10.0. Currents are shown without leak correction. To minimize pH<sub>i</sub> changes caused by large H<sup>+</sup> fluxes, pulses for large depolarizations in pulse families were sometimes shortened.

The reversal potential ( $V_{rev}$ ) was determined by two methods, depending on the relative positions of  $V_{rev}$  and the threshold voltage for activation of the  $g_{H^+}$ ,  $V_{threshold}$ . For constructs in which  $V_{threshold}$  was positive to  $V_{rev}$ , the latter was determined by examining tail currents. Because hH<sub>V1</sub> currents were the only time-dependent conductance present,  $V_{rev}$  was established by the amplitude and direction of current decay during deactivation. By using this procedure, time-independent leak or other extraneous conductances do not affect  $V_{rev}$  (Morgan and DeCoursey, 2014). Tail currents were not observed in nontransfected cells. For mutants in which  $V_{threshold}$  was negative to  $V_{rev}$  it was possible to observe directly the reversal of currents activated during pulse families.

Proton current amplitude ( $I_H$ ) was usually determined by fitting the rising current with a single exponential and extrapolating to infinite time. Proton conductance ( $g_H$ ) was calculated from  $I_H$  and  $V_{rev}$  measured in each solution:  $g_H = I_H / (V - V_{rev})$ . In some cases where current activation kinetics was difficult to evaluate,  $g_H$  was calculated from tail current amplitudes instead of  $I_H$ .

To evaluate  $\Delta$ pH dependence, it is necessary to establish the position of the  $g_H$ - $V$  relationship. For this purpose, we have adopted the voltage at which the  $g_H$  is 10% of its maximal value as a function of pH ( $V_{g_H, max/10}$ ), in preference to other parameters that have been used, such as the midpoint of a Boltzmann distribution or the threshold for activating detectable H<sup>+</sup> current,  $V_{threshold}$ . Because the  $g_H$ - $V$  relationship is steepest at low voltages, fairly large errors in estimating the maximum  $g_H$  ( $g_{H, max}$ ) produce only small errors in  $V_{g_H, max/10}$ . This parameter choice avoids the necessity of arbitrarily forcing nonsigmoidal  $g_H$ - $V$  data to fit a Boltzmann function (Musset et al., 2008a) or, alternatively, the need to identify the elusive threshold of channel activation,  $V_{threshold}$ , which is subjective and can be difficult when it occurs near  $E_H$ . Nevertheless,  $V_{threshold}$  remains useful as a supplemental parameter because its measurement requires minimal current flow and consequently produces negligible pH changes.

### Online supplemental material

Fig. S1 shows the sequence of the S4 segment in hH<sub>V1</sub>, kH<sub>V1</sub>, and EhH<sub>V1</sub>, illustrating the conserved Trp in the signature sequence that defines H<sub>V1</sub>, RxWRxxR. Fig. S2 shows saturation of the  $\Delta$ pH dependence of WT kH<sub>V1</sub> (from the dinoflagellate *Karlodinium veneticum*) and of the W176F mutant of kH<sub>V1</sub>. Fig. S3 shows the saturation of the  $\Delta$ pH dependence of WT EhH<sub>V1</sub> (from the coccolithophore *Emiliania huxleyi*) and of W278X mutants of EhH<sub>V1</sub>. The online supplemental material is available at <http://www.jgp.org/cgi/content/full/jgp.201511456/DC1>.

## RESULTS

The  $\Delta\text{pH}$  dependence of gating in hH<sub>V</sub>1 saturates above pH 8

Perhaps the most remarkable property of H<sub>V</sub>1 is the phenomenon of  $\Delta\text{pH}$ -dependent gating. We define  $\Delta\text{pH}$ , the transmembrane pH gradient, as  $\text{pH}_o - \text{pH}_i$ . Like other voltage-gated ion channels, H<sub>V</sub>1 opens upon depolarization, but the position of the  $g_{\text{H}}-V$  relationship is strongly and equally modulated by both  $\text{pH}_o$  and  $\text{pH}_i$ , shifting 40 mV for a unit change in either (Cherny et al., 1995). The set point of this relationship is positioned so that the human channel under normal conditions opens only when the electrochemical gradient is outwards. The practical consequence is that channel opening extrudes acid from the cell, which is essential to most of the functions of H<sub>V</sub>1.

Fig. 1 illustrates  $\Delta\text{pH}$ -dependent gating of the WT hH<sub>V</sub>1. Families of currents recorded in the same cell at four  $\text{pH}_o$  with  $\text{pH}_i$  7 are shown in Fig. 1 (A–D). Channel opening is characteristically slow, especially at lower  $\text{pH}_o$ . Examination of the corresponding  $g_{\text{H}}-V$  (proton conductance–voltage) relationships derived from these currents reveals a  $-40\text{-mV/U}$  pH shift as  $\text{pH}_o$  increases (Fig. 1 E). However, the shift between  $\text{pH}_o$  8 and  $\text{pH}_o$  9

is decidedly less than  $-40\text{ mV}$ . Saturation of the shift of the  $g_{\text{H}}-V$  relationship has not previously been identified in WT H<sub>V</sub>1 at either high or low  $\text{pH}_i$  or  $\text{pH}_o$ . A  $<40\text{-mV}$  shift between  $\text{pH}_o$  8 and 9 was noted previously and proposed to reflect the approach of  $\text{pH}_o$  to the  $\text{pK}_a$  of a site that senses  $\text{pH}_o$  (Cherny et al., 1995). This interpretation was later questioned when  $V_{\text{rev}}$  was found to deviate substantially from  $E_{\text{H}}$  at extreme  $\text{pH}_o$  values ( $\text{pH}_o$  9–10), and speculatively reinterpreted as reflecting loss of  $\text{pH}_i$  control at high pH, perhaps because of  $\text{OH}^-$  transport in rat alveolar epithelial cells (DeCoursey and Cherny, 1997). In the present study, we will show that the attenuation of  $\Delta\text{pH}$ -dependent gating constitutes genuine saturation, because it occurs at a pH where the channel is unequivocally proton selective and  $\text{pH}_i$  is well established (Fig. 4).

Fig. 1 (G–J) shows WT hH<sub>V</sub>1 currents at several  $\text{pH}_i$  measured in an inside-out patch of membrane, a configuration that allows changing  $\text{pH}_i$ . Again, activation (channel opening) is slow, increasingly so at high  $\text{pH}_i$  where the currents become smaller, presumably reflecting the rarity of permeant ions ( $1\text{ nM H}^+$  at pH 9). Corresponding  $g_{\text{H}}-V$  relationships plotted in Fig. 1 F exhibit a  $40\text{-mV/U}$  shift as  $\text{pH}_i$  increases, but also reveal that the shift appears to saturate between  $\text{pH}_i$  8 and  $\text{pH}_i$  9. Our

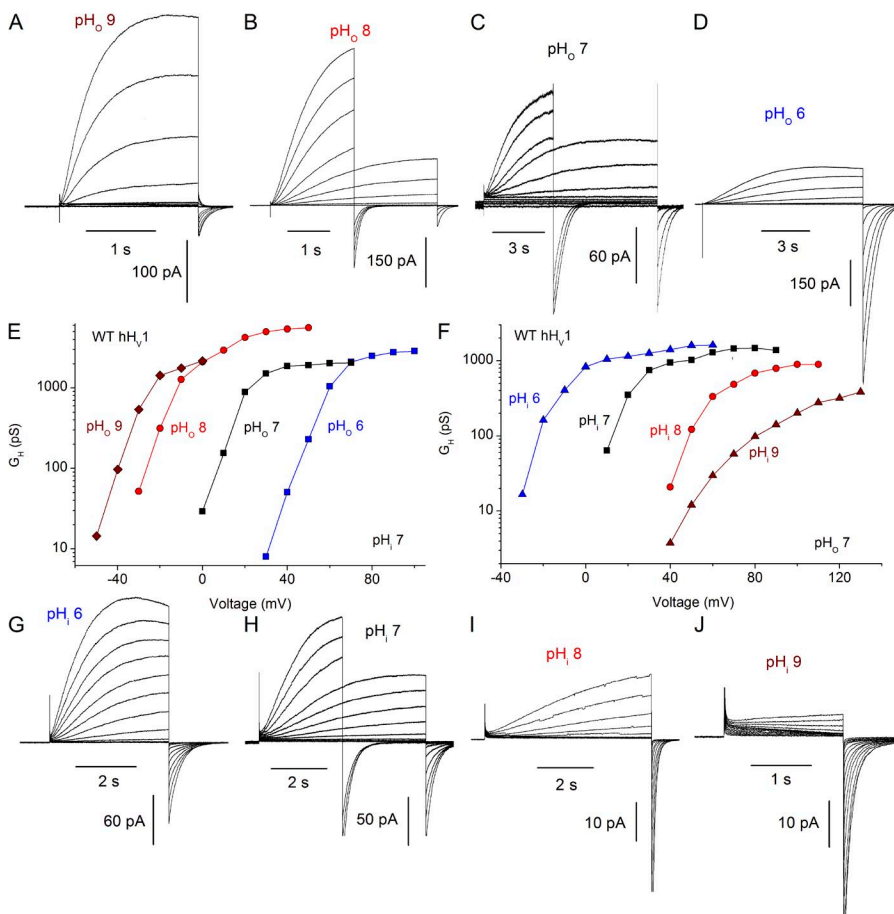


**Figure 1.** The  $\Delta\text{pH}$  dependence of WT hH<sub>V</sub>1 saturates at high  $\text{pH}_o$  or  $\text{pH}_i$ . (A–D) Families of currents at several  $\text{pH}_o$  are illustrated in a COS-7 cell expressing WT hH<sub>V</sub>1 with  $\text{pH}_i$  7 at holding potentials of  $-80$  (A),  $-60$  (B), or  $-40$  mV (C and D). In some families, shorter pulses were applied for large depolarizations to minimize proton depletion. (E) The  $g_{\text{H}}-V$  relationships are plotted, showing that the shift between  $\text{pH}_o$  8 and 9 is distinctly  $<40\text{ mV}$ . Measured  $V_{\text{rev}}$  in A–D was  $-95$ ,  $-53$ ,  $5$ , and  $57$  mV, respectively. (G–J) Current families in an inside-out patch are shown, with pipette  $\text{pH}_o$  7 and holding potentials of  $-60$  (G),  $-40$  mV (H and I), and  $-20$  mV (J), with  $g_{\text{H}}-V$  relationships plotted in F. Measured  $V_{\text{rev}}$  in G–J was  $-54$ ,  $0$ ,  $60$ , and  $115$  mV, respectively. For  $g_{\text{H}}$  calculation, the current amplitude  $I_{\text{H}}$  was obtained by fitting rising currents to a single-exponential function, with the exception of J, where because of the difficulty of fitting the slowly activating inward and outward currents, the tail current amplitude was used.

standard procedure is to extrapolate single-exponential fits to obtain “steady-state” current amplitudes. Because the currents in this patch at  $\text{pH}_i$  9 were small and activation was exceptionally slow, the  $g_H$  was derived from tail currents, which underestimates the  $g_H$ . However,  $V_{\text{threshold}}$  was the same at  $\text{pH}_i$  9 as for  $\text{pH}_i$  8, indicating a small  $g_H$ - $V$  shift. Quantitative values for these shifts are presented later (Figs. 3 and 4). Thus, saturation of  $\Delta\text{pH}$ -dependent gating occurs in WT hHv1, and it occurs at roughly the same absolute pH whether internal or external pH is varied. The simplest mechanistic explanation is that  $\Delta\text{pH}$  dependence is caused by titration of a site with  $\text{pK}_a$  of  $>8$  that is accessible from either side of the membrane. In the first (and only) model proposed to explain  $\Delta\text{pH}$ -dependent gating (Cherny et al., 1995), the same group(s) sensed  $\text{pH}_i$  and  $\text{pH}_o$  but was (were) required to be accessible only to one side of the membrane at a time. The data on WT hHv1 up to this point are consistent with this idea, which invokes a single pH-sensing site that has alternating access.

#### Mutations to Trp<sup>207</sup> in hHv1 compromise $\Delta\text{pH}$ -dependent gating

We replaced the bulky Trp<sup>207</sup> in the human proton channel, hHv1, with Ala, Phe, or Ser, designating the mutants W207A, W207F, and W207S, respectively. All mutants generated similar voltage- and time-dependent currents. Because we could not distinguish among the properties of these three mutants, their data are combined in data summaries and termed “W207X.” Families of currents recorded in the W207A mutant at four  $\text{pH}_o$  in Fig. 2 (A–D) reveal several noteworthy differences from WT hHv1. Most prominently, channel opening was two orders of magnitude faster, as will be described below (Fig. 5). Also evident is that the absolute position of the  $g_H$ - $V$  relationship tended to be more negative, resulting in pronounced inward currents at lower  $\text{pH}_o$  (Fig. 2, C and D), also evident in the current–voltage relationships (Fig. 2 E). The voltage at which the  $g_H$  was 10% of its maximal value,  $g_{H,\text{max}}$ , in whole-cells and inside-out patches at symmetrical pH 7.0 was variable but averaged  $9.8 \pm 2.6$  mV (mean  $\pm$  SEM;  $n = 14$ ) in

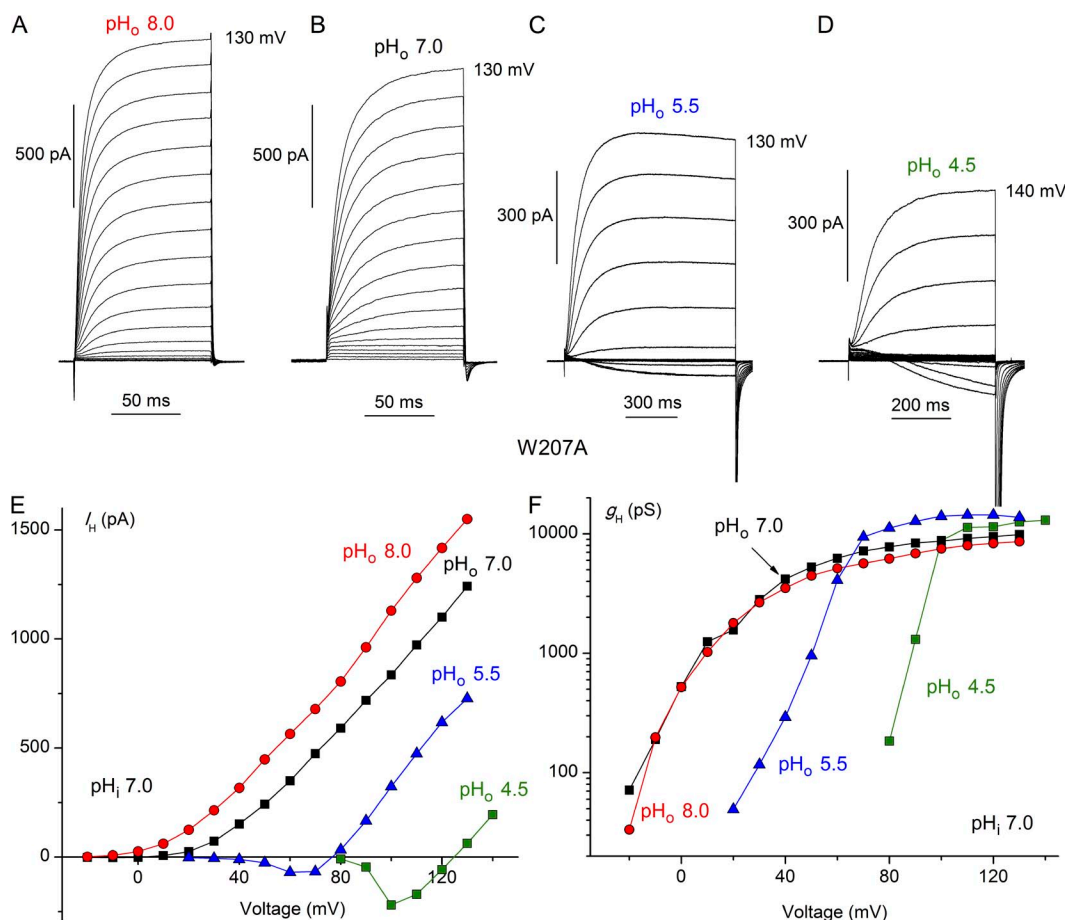


**Figure 2.** Modified  $\text{pH}_o$  sensitivity of W207A mutant hHv1. Families of proton currents at several  $\text{pH}_o$  in a cell with  $\text{pH}_i$  7.0 are illustrated (A–D). Pulses were applied in 10-mV increments up to the voltage indicated, from a holding potential of  $-60$  (A) or  $-40$  mV (B–D). (E) Proton current amplitudes ( $I_H$ ) from the cell in A–D were obtained by fitting the rising current with a single exponential and extrapolating to infinite time. (F) Proton conductance ( $g_H$ ) was calculated from the currents in E using  $V_{\text{rev}}$  measured in each solution.



WT hH<sub>V</sub>1 and  $-8.1 \pm 3.3$  mV ( $n = 20$ ) in W207X mutants ( $P < 0.001$ ).

More subtly, although voltage-dependent gating was shifted negatively by increases in pH<sub>o</sub> (Fig. 2, E and F), as in all known H<sub>V</sub>1, closer inspection reveals that the hallmark  $\Delta$ pH dependence is altered in Trp<sup>207</sup> mutants. When pH<sub>o</sub> was increased from 4.5 to 5.5 to 7.0, the ubiquitous 40-mV/U shift in the  $g_{H}$ - $V$  relationship (Cherny et al., 1995; DeCoursey, 2003) occurred (Fig. 2 F). However, above pH<sub>o</sub> 7.0, there was no further shift; thus, saturation of the shift occurred at  $\sim 1.5$  U lower pH<sub>o</sub> than in WT (Fig. 1 E). If the mechanism by which  $\Delta$ pH-dependent gating occurs involves one or more titratable groups, as has been proposed (Cherny et al., 1995), then replacement of Trp<sup>207</sup> apparently lowers the effective  $pK_a$  of this group(s).

To provide a more concise and quantitative way to evaluate  $\Delta$ pH dependence, in Fig. 3 we plot the voltage at which the  $g_{H}$  is 10% of its maximal value ( $V_{g_{H,max}/10}$ ) as a function of pH (discussed in Materials and methods). Fig. 3 (A and B) reiterates the observation from Fig. 1 that pH<sub>o</sub> and pH<sub>i</sub> dependence of gating both change

with a slope of 40 mV/U (dashed reference lines in all figures) over a wide range of pH, and both saturate between pH 8 and 9 in WT hH<sub>V</sub>1. An important additional result is that Fig. 3 (A and B) indicates that the saturation with pH<sub>o</sub> or pH<sub>i</sub> occurs independently of pH<sub>i</sub> or pH<sub>o</sub>, respectively. Thus, for example, in Fig. 3 B saturation occurred similarly above pH<sub>i</sub> 8 at either pH<sub>o</sub> 7 or 8. Evidently, saturation occurs at a particular absolute pH<sub>o</sub> or pH<sub>i</sub>, rather than at a particular  $\Delta$ pH. This result is consistent with the titration of one or more specific protonation sites that sense pH on only one side of the membrane. Hence, this result contradicts the simplest mechanism of a single site with alternating access to both sides of the membrane.

Analogous plots for the Trp<sup>207</sup> mutants (Fig. 3 C) show that their pH<sub>o</sub> dependence is fully saturated at pH<sub>o</sub>  $\geq 7.0$ , at least 1 U lower than in WT, with no further shift of the  $g_{H}$ - $V$  relationship up to pH<sub>o</sub> 10, confirming the impression from Fig. 2. Notably, the pH<sub>i</sub> dependence did not saturate up to pH<sub>i</sub> 8 (Fig. 3 D), and thus in contrast to WT, the saturating pH differs for pH<sub>o</sub> and pH<sub>i</sub> in the Trp<sup>207</sup> mutants. This result also speaks

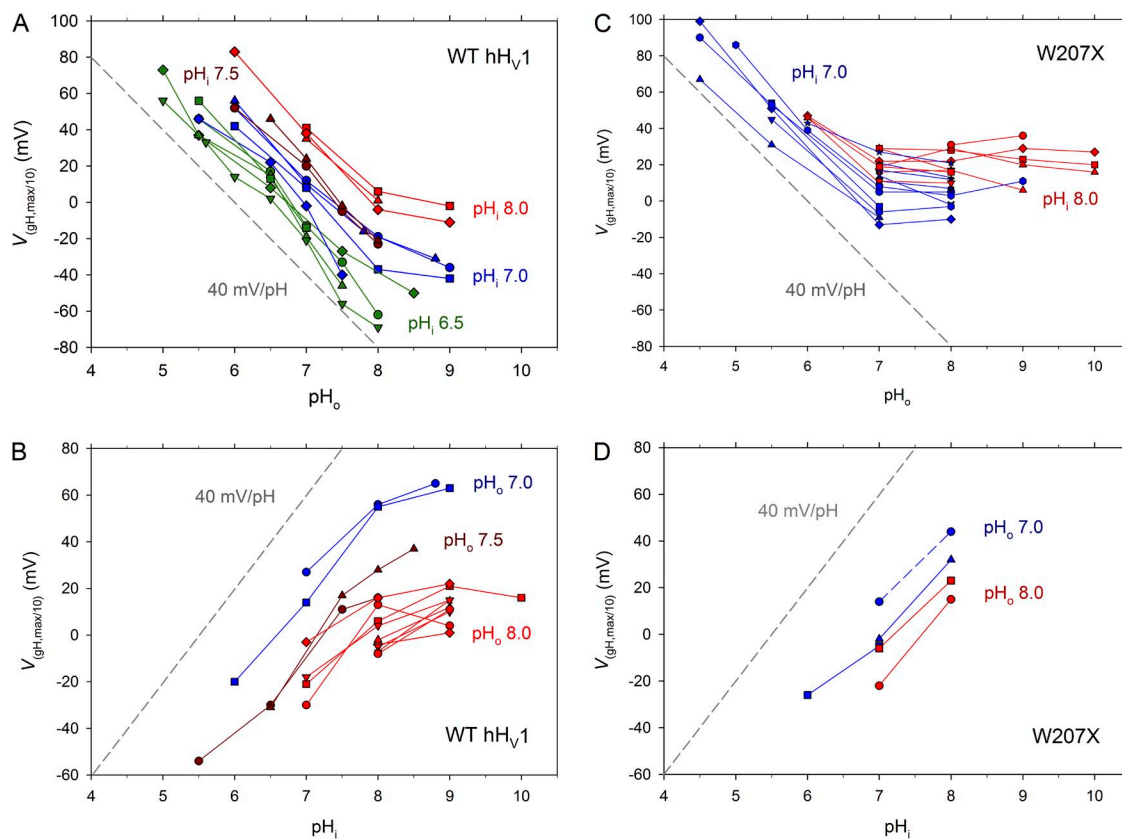


**Figure 3.** Saturation of the  $\Delta$ pH dependence of WT hH<sub>V</sub>1 (A and B) and of W207X mutants of hH<sub>V</sub>1 (C and D). The voltage at which  $g_{H}$  is 10% maximal ( $V_{g_{H,max}/10}$ ) is plotted as a function of pH<sub>o</sub> (A and C) or pH<sub>i</sub> (B and D), with lines connecting measurements in the same cell. In whole-cell measurements, pH<sub>i</sub> is color coded, as indicated. In inside-out patches, pH<sub>o</sub> is color coded, as indicated. For reference, the dashed gray line in each graph shows the slope of the ubiquitous 40-mV/U  $\Delta$ pH shift in the  $g_{H}$ - $V$  relationship (Cherny et al., 1995; DeCoursey, 2003); the horizontal position of this line is arbitrary. (C) Data from 13 W207A, eight W207F, and two W207S cells. (D) Data from three W207A, one W207F, and one W207S patch. No differences were detected among the Trp replacements.

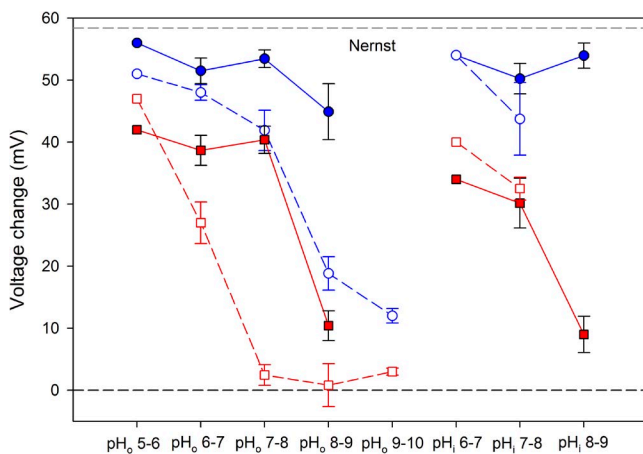


**Figure 4.** Saturation of  $\Delta\text{pH}$ -dependent gating occurs independently of loss of proton selectivity of  $\text{Trp}^{207}$  mutants. The mean  $\pm$  SEM (error bars) change in  $V_{\text{rev}}$  for a 1-U change in pH is plotted for WT hHv1 (closed blue circles) and for W207X (open blue circles). The shift in  $V_{\text{gH,max}/10}$  in the same cells is also plotted for WT hHv1 (closed red squares) and for W207X (open red squares). Numbers of cells for both parameters are one, six, eight, and five for increasing  $\text{pH}_o$  in WT; one, six, and eight for increasing  $\text{pH}_i$  in WT; one, five, 11, six, and three for increasing  $\text{pH}_o$  in W207X; and one and four for increasing  $\text{pH}_i$  in W207X. The difference in  $V_{\text{rev}}$  in W207X versus WT was significant at  $\text{pH}_o$  7–8 ( $P < 0.02$ ) and 8–9 ( $P < 0.001$ ). The difference in  $V_{\text{gH,max}/10}$  in W207X versus WT was significant at  $\text{pH}_o$  6–7 ( $P < 0.02$ ) and 7–8 ( $P < 0.0001$ ).

against the idea that the same group might sense pH on both sides of the membrane (with alternating access), because in the  $\text{Trp}^{207}$  mutants, the  $\text{pK}_a$  of the site(s) that sense  $\text{pH}_o$  and  $\text{pH}_i$  differ. An alternative interpretation that cannot be formally ruled out is that moving a single group to a different local environment might itself alter

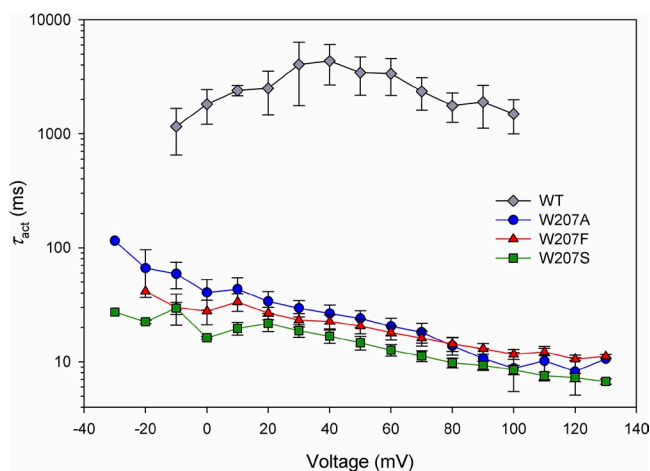


**Figure 5.** Replacement of  $\text{Trp}^{207}$  greatly accelerates hHv1 opening. The activation time constant,  $\tau_{\text{act}}$ , was obtained by fitting rising currents to a single exponential. All measurements were done at symmetrical pH 7.0 but include both whole-cell and excised inside-out patch data. Error bars represent mean  $\pm$  SEM, with  $n = 7, 9,$  and  $8$  for W207F, W207S, and W207A, respectively; WT includes five cells and seven inside-out patches.

its  $\text{pK}_a$ . In any event, the presence or absence of  $\text{Trp}^{207}$  evidently modulates either the accessibility of the pH-sensing site to the external solution or the effective  $\text{pK}_a$  of the site(s), or both.

A different analysis of the data is shown in Fig. 4. Solid red squares show that the change in  $V_{\text{gH,max}/10}$  for a 1-U change in  $\text{pH}_o$  or  $\text{pH}_i$  in WT is roughly 40 mV, but it drops precipitously to  $\sim 10$  mV at  $\text{pH}_o$  or  $\text{pH}_i$  8–9. For W207X (open red squares), the shift is already depressed at  $\text{pH}_o$  6–7 and is abolished (drops to  $\sim 0$  mV) at higher  $\text{pH}_o$  (7–8, 8–9, and 9–10). In contrast, the W207X mutants exhibit no loss of  $\Delta\text{pH}$  dependence up to  $\text{pH}_i$  7–8, emphasizing that the W207X mutation appears to selectively alter  $\text{pH}_o$  but not  $\text{pH}_i$  sensing. This result supports the idea of distinct external and internal pH sensors.

#### Mutations to $\text{Trp}^{207}$ in hHv1 facilitate channel opening

Another distinctive consequence of replacing  $\text{Trp}^{207}$  was faster channel opening, evident in Fig. 2. The turn-on of current during depolarizing pulses reflects the time course of channels opening. The rising currents were fitted with a single exponential to obtain  $\tau_{\text{act}}$ , the time constant of activation (channel opening). Mean  $\tau_{\text{act}}$  values plotted in Fig. 5 show that channel opening was  $\sim 100$  times faster than WT for each of the  $\text{Trp}^{207}$  mutants. WT kinetics was more variable than that of any of the mutants, perhaps reflecting the stronger temperature sensitivity of WT H<sub>v</sub>1 (DeCoursey and Cherny, 1998; Kuno et al., 2009) or variable proton depletion during the much longer pulses required to determine

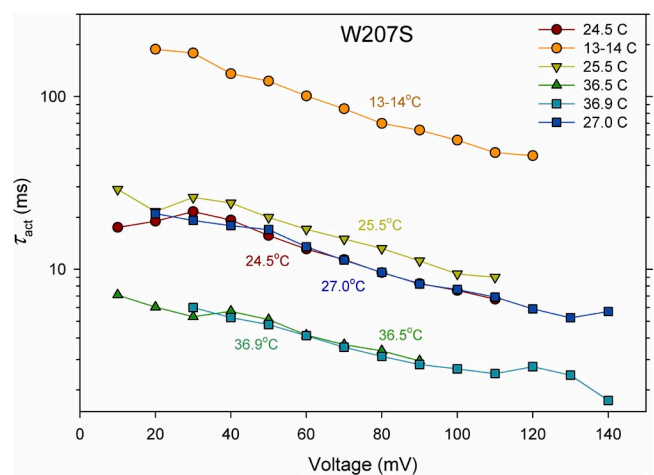


**Figure 6.** Replacement of  $\text{Trp}^{207}$  decreases the Arrhenius activation energy for hHv1 opening. The activation time constant,  $\tau_{\text{act}}$ , was determined in one cell during families of pulses at various temperatures at symmetrical pH 7. The sequence is indicated in the inset. The  $Q_{10}$  was somewhat higher at lower voltages (e.g., 4.3 at 20 mV and 3.7 at 100 mV, for the entire temperature range). As reported previously for native H<sub>v</sub>1 (DeCoursey and Cherny, 1998),  $E_a$  also increased at lower temperatures. Temperature drift during families of pulses was on the order of  $1^\circ\text{C}$ .

WT kinetics. Surprisingly, replacement of Trp with an aliphatic hydrophobic residue (Ala), a polar hydrophilic residue (Ser), or an aromatic residue (Phe) produced identically profound acceleration of activation. The kinetic consequences of Trp at position 207 appear to be unique and unrelated to such generic qualities as hydrophobicity, polarity, or aromaticity.

Channel-closing kinetics was examined by measuring  $\tau_{\text{tail}}$ , the time constant of tail current decay (deactivation). Measured at symmetrical pH 7.0 at  $-40$  mV,  $\tau_{\text{tail}}$  was  $227 \pm 22$  ms ( $n = 16$ ) in WT hHv1 and 29 times faster in the three Trp<sup>207</sup> mutants ( $7.8 \pm 0.8$  ms;  $n = 17$ ).

If the slowing of gating by Trp<sup>207</sup> were rate determining in WT channels, then the activation energy,  $E_a$  for gating should be lower in mutants than the 30–38 kcal/mol in WT channels (DeCoursey and Cherny, 1998). Fig. 6 illustrates that this was the case. The time constant of channel opening ( $\tau_{\text{act}}$ ) was determined by fitting rising currents with a single-exponential function in current families recorded at several temperatures. The Arrhenius activation energy,  $E_a$ , was calculated from  $E_a = RT_1T_2/(T_2 - T_1) \ln(\tau_{\text{act},1}/\tau_{\text{act},2})$ , where  $R$  is the gas constant ( $1.9872$  cal K<sup>-1</sup> mol<sup>-1</sup>) and  $T_1$  and  $T_2$  are the lower and higher temperatures (in K) (DeCoursey and

Cherny, 1998). In three experiments (two whole cell and one inside-out patch),  $E_a$  determined over the entire temperature range from 11–13 to 35–37°C averaged  $\sim 22$  kcal/mol. Therefore, the process involved in slow WT activation that is regulated by Trp<sup>207</sup> is rate limiting.

Mutations to Trp<sup>207</sup> in hHv1 compromise proton selectivity Central to performing all of the functions of Hv1 is its perfect proton selectivity. Proton selectivity was evaluated by measuring the reversal potential,  $V_{\text{rev}}$ , at various pH. Because replacing Trp<sup>207</sup> shifted the  $g_{\text{H}}-V$  relationship negatively, at some  $\Delta\text{pH}$ ,  $V_{\text{rev}}$  could be observed directly as reversal of the current during families of pulses, as illustrated in Fig. 7 (A and C). Alternatively,  $V_{\text{rev}}$  can be estimated in the usual manner using tail currents (Fig. 7, E and F). Surprisingly, there was only a small shift in  $V_{\text{rev}}$  ( $<20$  mV) between pH<sub>o</sub> 8 and 9 in the W207F mutant (Fig. 7, E and F). In comparison, the same pH<sub>o</sub> change produced a nearly Nernstian (58-mV) shift in the WT hHv1 (Fig. 7, G and H). The replacement of Trp<sup>207</sup> compromised proton selectivity.

Fig. 8 A confirms the proton specificity of the WT hHv1. The reversal potential,  $V_{\text{rev}}$ , measured over a wide range of pH<sub>o</sub> (5.0–9.0) and pH<sub>i</sub> (5.5–9.0) was close to

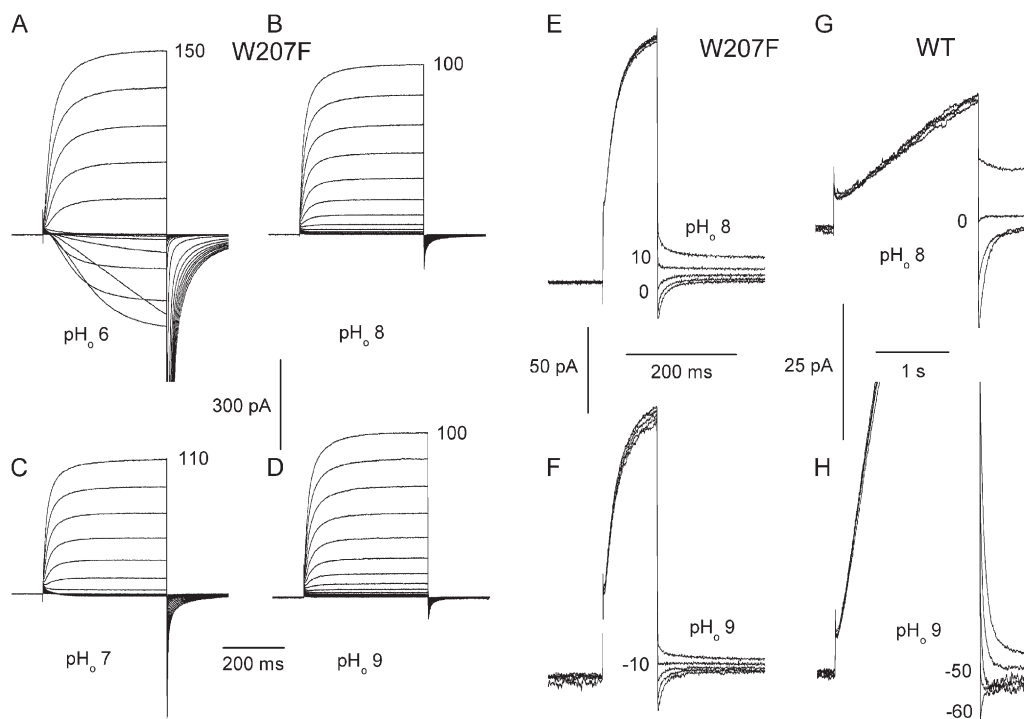


**Figure 7.** Measurement of  $V_{\text{rev}}$  in W207F and in WT hHv1. (A–D) Families of currents in a cell expressing W207F channels were elicited by depolarizing pulses applied in 10-mV increments up to the voltage shown. When it is positive to  $V_{\text{threshold}}$ ,  $V_{\text{rev}}$  is easily obtained by interpolating between inward and outward currents, as in families at pH<sub>o</sub> 6 (A) or 7 (C). In the same cell at pH<sub>o</sub> 8 (B and E) and 9 (D and F),  $V_{\text{rev}}$  was extracted from the reversal of tail currents. In this cell,  $V_{\text{rev}}$  at pH<sub>o</sub> 6, 7, 8, and 9 was 102, 52, 7, and  $-10$  mV;  $E_{\text{H}}$  was 117, 58, 0, and  $-58$  mV, respectively. Loss of proton selectivity is indicated by the large deviation of  $V_{\text{rev}}$  from  $E_{\text{H}}$  at high pH<sub>o</sub>. In WT hHv1, the shift in  $V_{\text{rev}}$  obtained by tail currents at pH<sub>o</sub> 8 (G) and 9 (H) was nearly Nernstian. Both cells in this figure contained pH<sub>i</sub> 8 solutions. The holding potential was  $-20$  (G),  $-30$  (C),  $-40$  (A, B, E, and H), or  $-60$  mV (D and F). Prepulses were to 60 (E and F), 20 (G), or 10 mV (H).

the Nernst potential,  $E_H$ , shown as a dashed line. Surprisingly, Trp<sup>207</sup> mutants were imperfectly proton selective. Fig. 8 B shows that although they were highly selective at neutral and acidic pH, at high pH<sub>o</sub> (8–10), the measured reversal potential,  $V_{rev}$ , deviated consistently and substantially from  $E_H$ .

The mean shift in  $V_{rev}$  for a 1-U change in pH is plotted in Fig. 4 (blue circles). The  $V_{rev}$  of WT hH<sub>V</sub>1 (closed blue circles) was reasonably near  $E_H$  at all pH studied, whereas  $V_{rev}$  of the W207X mutants (open blue circles) was distinctly sub-Nernstian at pH<sub>o</sub> 8–10, being significantly lower than WT at pH<sub>o</sub> 7–8 and 8–9. Trp<sup>207</sup> mutation produces loss of proton selectivity, but only at high pH<sub>o</sub>.

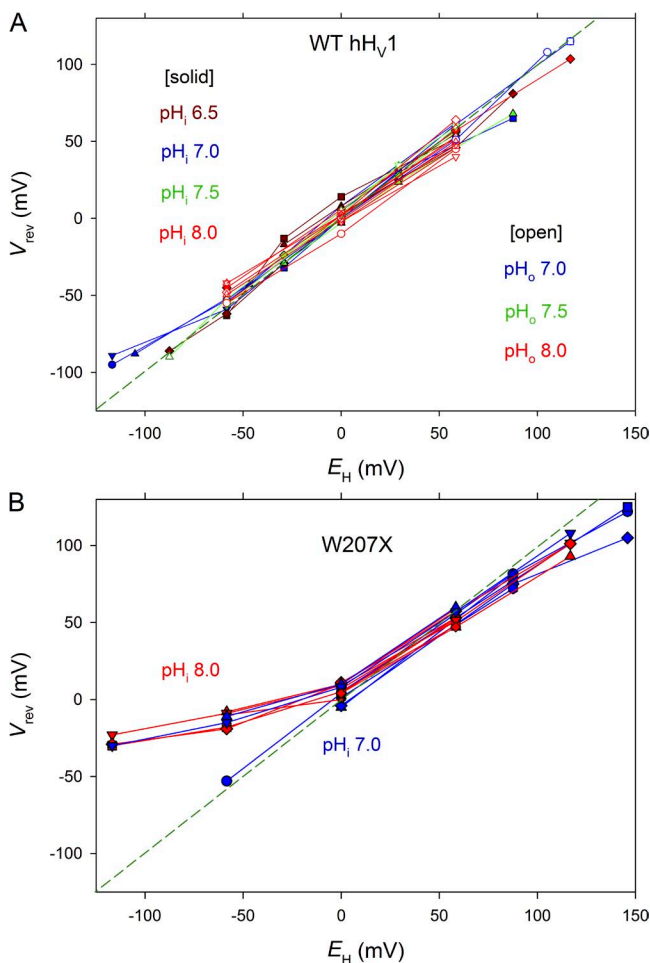


**Figure 8.** Proton selectivity is perfect in WT hH<sub>V</sub>1 (A) but compromised in Trp<sup>207</sup> mutants (B). Proton selectivity is indicated by the proximity of measured values of  $V_{rev}$  and the Nernst potential for H<sup>+</sup>,  $E_H$ . Data were obtained in whole-cell (closed symbols) and inside-out patch configuration (open symbols). In whole-cell measurements, the color-coded  $pH_i$  solution was in the pipette, and  $pH_o$  was varied, with lines connecting measurements in each cell. In inside-out patch measurements,  $pH_o$  was the pipette solution and  $pH_i$  was varied. Whole-cell measurements in B include eight W207F, 12 W207A, and one W207S cell. For W207X mutants, currents in patches were too small to allow reliable estimation of  $V_{rev}$ .

#### Replacement of Trp in a dinoflagellate H<sub>V</sub>1 (kH<sub>V</sub>1) speeds activation

Given that replacing Trp greatly speeds activation in hH<sub>V</sub>1, we were curious as to whether the same would be true in other species. To make this test rigorous, we selected an evolutionarily distant species in which the amino acid identity with hH<sub>V</sub>1 is only 15%, namely *K. veneficum* (Smith et al., 2011). We made the same three substitutions to the corresponding Trp<sup>176</sup> in kH<sub>V</sub>1 (Fig. S1): W176A, W176F, and W176S. These mutants generated proton-selective currents in the pH range explored that exhibited qualitatively similar changes when pH<sub>o</sub> was changed (Fig. 9, A vs. B, and C vs. D). Like their human counterparts, the Trp mutants activated extremely rapidly. Activation time constants were nearly two orders of magnitude faster than in the WT channel (Fig. 9 E). WT closing kinetics was faster in kH<sub>V</sub>1 than in hH<sub>V</sub>1, and in the Trp<sup>176</sup> mutants, tail current decay was often too fast to distinguish reliably from capacity transients. Mirroring the pattern seen in the human Trp mutants,  $\tau_{act}$  was roughly the same whether Trp<sup>176</sup> was replaced by Ser, Ala, or Phe (Fig. 9 E). The same remarkable result obtained in both species is that Trp in the signature sequence (RxWRxxR) profoundly slows channel opening by a mechanism that other amino acids tested are unable to replicate. This result suggests a quite specific type of interaction.

The kH<sub>V</sub>1 channel does exhibit  $\Delta pH$ -dependent gating, although its absolute voltage range of opening is 60 mV more negative than in other species (Smith et al., 2011). Therefore, it was of interest to determine whether saturation of this effect occurs. In WT kH<sub>V</sub>1, saturation was observed above pH<sub>o</sub> 8.0 or  $pH_i$  8.0 (Fig. S2), similar to the pH at which saturation occurs in WT hH<sub>V</sub>1. Also like hH<sub>V</sub>1, Trp mutation compromised  $\Delta pH$  dependence, with saturation occurring at lower pH<sub>o</sub> in the W176F mutant (Fig. S2 C).

#### Replacement of Trp in a coccolithophore H<sub>V</sub>1 (EhH<sub>V</sub>1) speeds activation and shifts the $g_H$ -V relationship negatively

To further test the generality of the roles of Trp, we produced analogous mutations in the coccolithophore, *E. huxleyi* H<sub>V</sub>1 (EhH<sub>V</sub>1), namely W278A, W278S, and W278F (Fig. S1). The EhH<sub>V</sub>1 sequence differs drastically from hH<sub>V</sub>1, with only 18% identity, as well as from kH<sub>V</sub>1, with 29% identity. Fig. 10 shows that activation kinetics was also faster in the EhH<sub>V</sub>1 when Trp<sup>278</sup> was replaced, although the effect was smaller than in the other species examined. Opening of these mutants was accelerated four- to sixfold in the positive voltage range.

Another pronounced change in EhH<sub>V</sub>1 mutants was a negative shift of the  $g_H$ -V relationship, with the voltage at which the  $g_H$  was 10% of  $g_{H,max}$  averaging  $-5.2 \pm 2.9$  (12) in WT EhH<sub>V</sub>1 and  $-33.4 \pm 2.3$  (14) in the mutants, a  $-28$ -mV shift. Some of the slowing of  $\tau_{act}$  may be



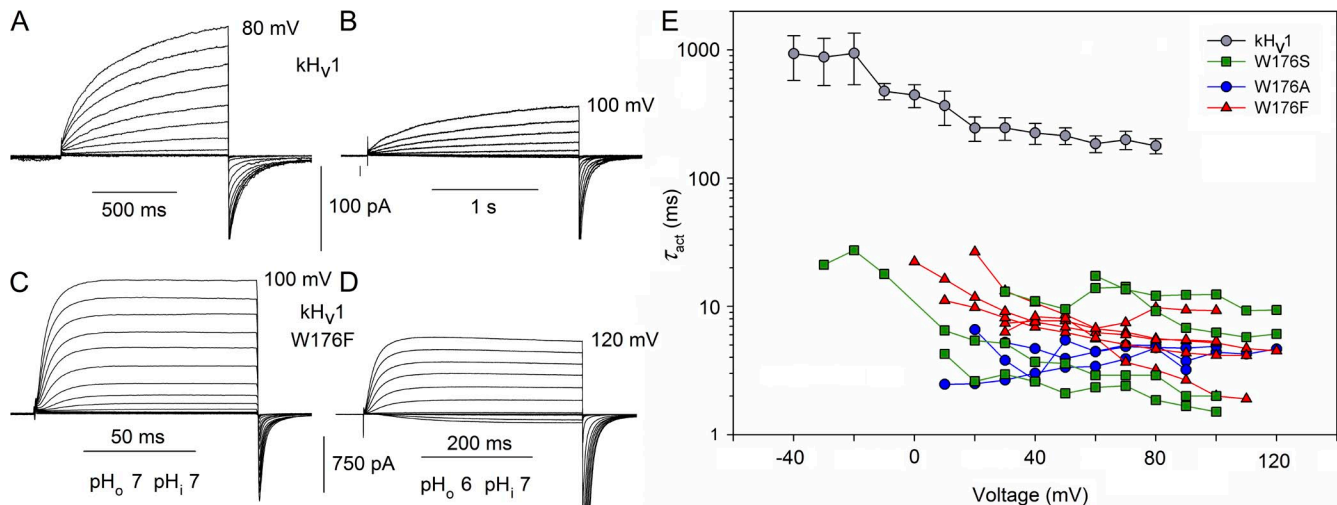


**Figure 9.** The W176F mutation in the dinoflagellate kHv1 accelerates channel opening. Families of currents in WT kHv1 (A and B) and in the W176F mutant (C and D), studied at pH<sub>o</sub> 7 (A and C) or 6 (B and D), as indicated, all at pH<sub>i</sub> 7. Note the different time scales. Voltage steps were applied in 10-mV increments to the final voltage indicated. The holding potential was  $-60$  (A and C) or  $-40$  mV (B and D). (E) Replacement of Trp<sup>176</sup> in the dinoflagellate kHv1 with Ala, Ser, or Phe hastens channel opening to the same extent. The activation time constant,  $\tau_{act}$ , was determined by fitting the turn-on of current with a single rising exponential. The WT channel kinetics (mean  $\pm$  SEM;  $n = 5-14$ ) was extracted from data for a previous study, all at symmetrical pH 7.0 (Smith et al., 2011). Single mutants, as indicated, were expressed in HEK-293 or COS-7 cells. Measurements were performed in whole-cell configuration at symmetrical pH 7. Data from each cell are connected by lines.

ascribable to this shift; the peak value of  $\tau_{act}$  occurs in a more negative voltage range in W278X than in WT.

Intriguingly, the  $\Delta$ pH dependence of EhHv1 appeared consistently steeper ( $\sim 50$  mV/U pH) both for changes in pH<sub>o</sub> and pH<sub>i</sub> than in Hv1 in other species (Fig. S3). Saturation of  $\Delta$ pH dependence was evident only above

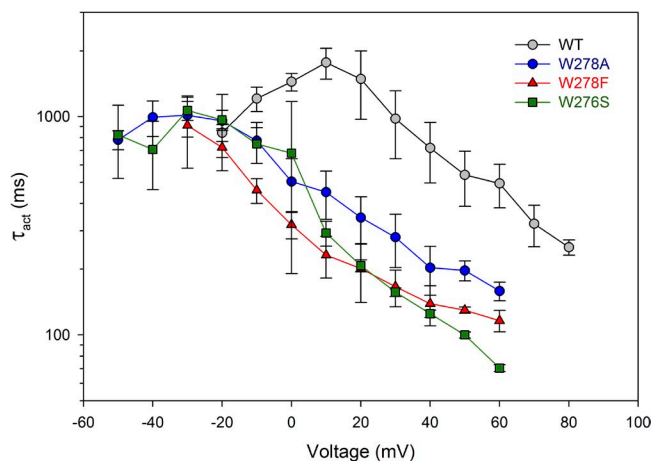


**Figure 10.** Replacement of Trp<sup>278</sup> in the coccolithophore EhHv1 with Ala, Ser, or Phe hastens channel opening to the same extent. The activation time constant,  $\tau_{act}$ , was determined by fitting the turn-on of current with a single rising exponential. The mean ratio of WT/W278X within the range of 10–60 mV was 3.5 (W278A), 5.7 (W278F), and 6.3 (W278S). Numbers of cells are: WT, three to six; W278A, three to four; W278F, two to four; W278S, two to three. Single mutants were expressed in HEK-293 or COS-7 cells, and measurements were performed in whole-cell configuration at symmetrical pH 7. Error bars represent mean  $\pm$  SEM.

pH<sub>o</sub> 8.0 in WT, essentially identical to both hHv1 and kHv1. No significant change in this property was detected in the EhHv1 mutants, although the mean shift from pH<sub>o</sub> 7 to pH<sub>o</sub> 8 decreased from  $-53 \pm 2$  mV (SEM;  $n = 4$ ) in WT to  $-43 \pm 5$  mV ( $n = 4$ ) in mutants. The  $\Delta$ pH dependence of EhHv1 would thus be maintained reasonably well over the normal pH range experienced by coccolithophores; the pH of seawater is 7.5–8.4 (Chester and Jickells, 2012). That saturation of  $\Delta$ pH-dependent gating occurred at the same pH<sub>o</sub> and pH<sub>i</sub> in all three species suggests that the same or similar group(s) may be involved in pH sensing.

## DISCUSSION

### Activation kinetics

*Cation- $\pi$  interaction between Trp<sup>207</sup> and Arg<sup>211</sup> in hHv1 latches the channel closed.* The most obvious effect of replacing Trp<sup>207</sup> with smaller amino acids was acceleration of channel opening by two orders of magnitude. The precise physical mechanism by which Trp slows WT Hv1 opening can only be speculated, but several possibilities exist. In the closed mHv1 structure (78% sequence identity to hHv1), Trp is oriented toward the lipid (Takeshita et al., 2014), suggesting that hydrophobic interactions might stabilize it in this position. Hydrophobic interactions with membrane lipids have been considered for closed-state stabilization by Val<sup>363</sup> in the *Shaker* K<sup>+</sup> channel VSD (Lacroix et al., 2013). However, the aromatic Phe, which engages in purely hydrophobic interactions (Killian and von Heijne, 2000),

does not share this behavior in  $H_{V1}$ . In all three species studied here, the Trp→Phe mutant did not exhibit intermediate behavior but rather activated as rapidly as Trp→Ser or Trp→Ala mutants. This result suggests that the ambivalence of Trp in having a polar amide group plays a key role. As discussed in the Introduction, the  $mH_{V1}$  structure (Takeshita et al., 2014) appears to indicate that Trp engages in cation– $\pi$  interaction with R3, stabilizing the closed structure. In fact, Trp<sup>207</sup> and Arg<sup>211</sup> are an example of the second most common cation– $\pi$  interaction that occurs within  $\alpha$  helices between residues  $i$  and  $(i + 4)$  (Gallivan and Dougherty, 1999).

The portion of  $mH_{V1}$  containing Trp and R3 is compared with the corresponding region in the *Ciona intestinalis* voltage-sensing phosphatase (CiVSP) in Fig. 11, with both proteins considered to be in their closed or “down” position. It seems surprising that in both structures, R3 appears to lack direct aqueous contact. Burying acidic or basic amino acids can shift their  $pK_a$  by as much as 5 pH units, but Arg is the most likely to remain ionized (Kim et al., 2005). In fact, Arg appears uniquely able to remain protonated inside proteins (Harms et al., 2011). In the down structure of CiVSP, R3 is found in a pocket surrounded by hydrophobic residues that faces away from the center of the VSD; the guanidinium group of R3 is oriented somewhat “sideways” to the plane of the lipid and it salt-bridges with Asp<sup>186</sup> (Fig. 11 A). In the  $mH_{V1}$  structure (Fig. 11 B), Trp<sup>203</sup> appears to provide part of a similar pocket in which R3 interacts both with Asp<sup>170</sup> (equivalent to Asp<sup>174</sup> in  $hH_{V1}$  and Asp<sup>186</sup> in CiVSP)

and with Asn<sup>210</sup>, although in this structure the guanidinium of R3 appears to be pointing nearly directly away from the center of the channel (Fig. 11 B). We speculate that Phe may be unable to stabilize R3 in this position, possibly because of Phe’s weaker cation– $\pi$  interaction capability. The electrostatic R3–Asp interaction in closed  $H_{V1}$  may also contribute a stabilizing function like that of the corresponding Lys<sup>374</sup>–Asp<sup>316</sup> in the closed *Shaker* K<sup>+</sup> channel VSD (Papazian et al., 1995). In all open  $H_{V1}$  models (Ramsey et al., 2010; Wood et al., 2012; Kulleperuma et al., 2013; Chamberlin et al., 2014), R3 has rotated to face the pore, whereas Trp still appears to face the lipid. For this kind of conformational change to occur during opening, the interactions between the Trp–Arg pair would have to be disrupted. The much more rapid opening in the W207X mutants may reflect the absence of these stabilizing interactions.

The faster activation kinetics after Trp mutation in  $hH_{V1}$  qualitatively resembles that seen in forced monomerization. Monomeric constructs open four to seven times faster than their dimeric counterparts (Koch et al., 2008; Tombola et al., 2008; Musset et al., 2010; Fujiwara et al., 2012). Might Trp mutation eliminate interaction at the dimer interface between Trps from each protomer that normally contribute to closed-state stabilization? This notion is contradicted by a cysteine cross-linking study indicating that the two S4 helices appear not to interact (Lee et al., 2008). On the other hand, the S4 segments are close to each other in a proposed dimer model based on the closed structure of  $mH_{V1}$  (Takeshita et al., 2014).

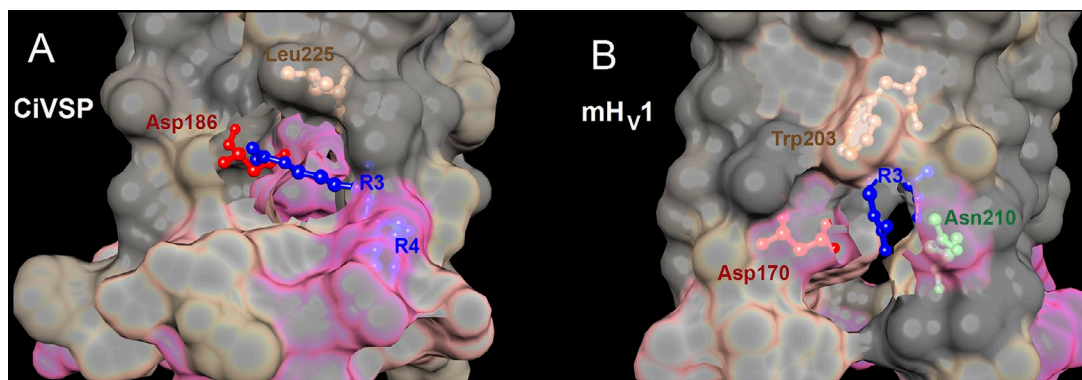


**Figure 11.** Crystal structures of CiVSP in the “down” state and  $mH_{V1}$  chimera in the closed state reveal pockets that enclose electrostatic interactions involving R3. The crystal structures of the down state of CiVSP (A) (Li et al., 2014) and the closed  $mH_{V1}$  chimera (B) (Takeshita et al., 2014) were superimposed with the same orientation. The top is toward the extracellular surface, and the view is from the side. The interfacial surface between protein and lipid is cut away to show the pocket containing R3 and its interacting partners. Local hydrophobicity is indicated by gray (hydrophobic), tan (intermediate), and pink (hydrophilic). (A) In the down structure of CiVSP (Protein Data Bank [PDB] accession no. 4G80), which is more closely related to  $H_{V1}$  phylogenetically than is the VSD of other ion channels (Smith et al., 2011), R3 faces away from the center of the VSD. The guanidinium group of R3 forms a salt-bridge with Asp<sup>186</sup>. (B) In the closed structure of  $mH_{V1}$  (PDB accession no. 3WKV), Trp<sup>203</sup> and R3 both face away from the center of the channel; the guanidinium of R3 appears to point nearly directly away from the center of the channel. In the  $mH_{V1}$  structure, Trp<sup>203</sup> forms the roof of the pocket, in which R3 interacts both with Asp<sup>170</sup> (equivalent to Asp<sup>174</sup> in  $hH_{V1}$  and Asp<sup>186</sup> in CiVSP) and with Asn<sup>210</sup>. Molecular graphics and analyses were performed with the University of California, San Francisco (UCSF), Chimera package (resource for Biocomputing, Visualization, and Informatics, UCSF, San Francisco; supported by NIGMS P41-GM103311) (Pettersen et al., 2004).

Is it possible that the primary reason for the conservation of Trp<sup>207</sup> is to slow gating? It is not immediately obvious why slow H<sub>V</sub>1 activation would be evolutionarily advantageous. On the other hand, rapid opening would not confer any advantage for most of the functions proposed for H<sub>V</sub>1 in mammalian cells. For example, H<sub>V</sub>1 is activated in phagocytes to compensate for the electrogenic activity NADPH oxidase (Henderson et al., 1987; DeCoursey et al., 2003); the latter enzyme is turned on by most stimuli only after a delay and on a time scale of seconds (DeCoursey and Ligeti, 2005). In cells in which acid extrusion via H<sub>V</sub>1 occurs for the purpose of pH homeostasis or signaling, such as airway epithelia (Fischer, 2012), basophils (Musset et al., 2008b), B lymphocytes (Capasso et al., 2010), neutrophils (Morgan et al., 2009), or sperm (Lishko et al., 2010), rapid opening is less important than simply remaining open as long as necessary. The absence of inactivation is thus arguably more critical than rapid activation would be. Another possibility is that because a single *HVCN1* gene codes for proton channels in a multiplicity of cell types in which H<sub>V</sub>1 serves diverse purposes, the properties of the protein must be compatible with the physiology of all cells. An excitable cell might be ill-served by a rapidly activating proton channel that could interfere with the action potential.

Trp<sup>207</sup> in hH<sub>V</sub>1 anchors the S4 segment and stabilizes the closed channel. By retarding channel opening by 100-fold, while slowing closing only 29-fold, Trp<sup>207</sup> might tend to produce a net stabilization of the closed state. In fact, Trp<sup>207</sup> mutants did activate at voltages 18 mV more negative than WT hH<sub>V</sub>1; therefore Trp<sup>207</sup> does contribute to stabilizing a closed state. Native proton channels open almost exclusively positive to  $E_H$  and thus never produce significant inward current (DeCoursey, 2003). The negative shift of the  $g_H$ - $V$  relationship in Trp<sup>207</sup> mutants resulted in distinct inward currents just above  $V_{\text{threshold}}$ , especially with inward H<sup>+</sup> gradients (e.g., Figs. 2, C-E, and 7, A and C). Substitution of Trp<sup>207</sup> thus subverts this principal feature of H<sub>V</sub>1 and compromises the task of proton extrusion. One could speculate that Trp<sup>207</sup> fine tunes the voltage dependence of H<sub>V</sub>1 to prevent premature opening. Because of the proximity of  $V_{\text{threshold}}$  and  $V_{\text{rev}}$  in WT H<sub>V</sub>1 (Cherny et al., 1995; Musset et al., 2008a), without the stabilization of the closed state by Trp<sup>207</sup>, channel opening would result in proton influx. Given that mammalian cells are largely concerned with extrusion of metabolically produced acid (Roos and Boron, 1981), such a propensity would be deleterious to cell homeostasis.

In EhH<sub>V</sub>1, Trp also decidedly stabilized the closed state; the  $g_H$ - $V$  relationship was 28 mV more negative in W278X mutants than in WT. In contrast, W176X mutants in kH<sub>V</sub>1 activated 25 mV more positively than WT. The atypical behavior of kH<sub>V</sub>1 in this regard may reflect

distinct teleological considerations. EhH<sub>V</sub>1 exists to extrude acid (Taylor et al., 2011), and like hH<sub>V</sub>1, must therefore be poised to open just above  $E_H$ . In contrast, kH<sub>V</sub>1 activates 60 mV more negatively than H<sub>V</sub>1 in any other species (Smith et al., 2011), which is ideal for its quite different function in dinoflagellates of mediating H<sup>+</sup> influx that triggers the flash in bioluminescent species (Fogel and Hastings, 1972). The molecular mechanism responsible for the unique kH<sub>V</sub>1 voltage dependence is unknown.

#### Temperature dependence

The gating kinetics of H<sub>V</sub>1 in several mammalian cells is extraordinarily temperature dependent, with  $Q_{10}$  values of 6–9 ( $E_a$  for the delay,  $\tau_{\text{act}}$ , and  $\tau_{\text{tail}}$  were identically 30–38 kcal/mol) (DeCoursey and Cherny, 1998). The Arrhenius activation energy,  $E_a$ , of channel opening ( $\tau_{\text{act}}$ ) of W207S was 20–25 kcal/mol ( $Q_{10}$  of 3.5–4.0), distinctly smaller than in WT, indicating that the factors that establish the kinetics in W-free H<sub>V</sub>1 have more modest  $E_a$ . Evidently, the perfectly conserved Trp<sup>207</sup> is the dominant contributor to the exotic temperature sensitivity of WT hH<sub>V</sub>1, and replacing it lowers the  $Q_{10}$  of gating into the range of most ordinary ion channels; two dozen examples are given in Table II of DeCoursey and Cherny (1998). That Trp is involved in the rate-limiting step in H<sub>V</sub>1 opening is consistent with the idea that opening a closed H<sub>V</sub>1 requires disrupting the cation- $\pi$  interactions between Trp and Arg, and perhaps also inter-protomer Trp-Trp interactions in the dimer that stabilize closed channels.

The gating kinetics of hH<sub>V</sub>1 is much slower than that of many voltage-gated channels; removing Trp eliminates this distinctive property as well. In WT hH<sub>V</sub>1, the activation time constant,  $\tau_{\text{act}}$ , is in the range of seconds at room temperature, but it plummets into the low millisecond range in Trp<sup>207</sup> mutants. Thus, in terms of both channel-opening kinetics and temperature dependence, the effect of removing Trp<sup>207</sup> is like Kryptonite, turning a Super-channel into an ordinary mortal channel.

#### Proton selectivity

Over a wide range of pH, the WT hH<sub>V</sub>1 appears to be perfectly selective. In a previous study, WT H<sub>V</sub>1 appeared to lose selectivity between pH 9 and 10 (DeCoursey and Cherny, 1997); the present study extended only up to pH 9. The Trp<sup>207</sup> mutants, however, lost selectivity at less extreme pH, beginning at pH<sub>o</sub> 8 (Figs. 4, 7, E and F, and 8 B). It is unlikely that this loss of proton selectivity reflects a direct participation of Trp in the selectivity mechanism. It is well established that an Asp in the S1 helix is crucial to proton selectivity (Musset et al., 2011; Smith et al., 2011). This Asp can be relocated from position 112 to 116 in hH<sub>V</sub>1 without loss of proton selectivity, but charge compensation by interaction with



one or more S4 Arg appears essential (Morgan et al., 2013). Recently, quantum mechanical calculations demonstrated an explicit mechanism by which Asp–Arg interaction is sufficient to produce proton-selective conduction without requiring contribution from the rest of the protein beyond providing a scaffold and focusing aqueous access to the selectivity filter (Dudev et al., 2015). If Trp helps anchor the S4 helix in the membrane, its removal may allow sufficient intramolecular movement to disrupt the Asp–Arg interaction that is critical to proton-selective conduction. That the loss of selectivity manifests only at high  $pH_o$  may reflect deprotonation of a cationic group that stabilizes the open channel.

#### Trp<sup>207</sup> is essential for normal $\Delta pH$ -dependent gating

Perhaps the most striking consequence of Trp mutation is the weakening of  $\Delta pH$ -dependent gating, a quintessential feature that provides the basis for  $H_V1$  function in all cells. In all species, and even among all known  $H_V1$  mutations described to date (Ramsey et al., 2010; Musset et al., 2011; DeCoursey, 2013), the  $g_{H-V}$  relationship shifts a roughly 40-mV/U change in  $\Delta pH$  over a wide range of  $pH_o$  and  $pH_i$ . With the single exception of the dinoflagellate *K. veneficum* (Smith et al., 2011), this behavior results in  $H_V1$  opening only when the electrochemical gradient is outwards, so that  $H_V1$  extrudes acid. The mechanism of  $\Delta pH$ -dependent gating remains one of the most elusive unsolved mysteries regarding  $H_V1$ . The first and only explicit model of  $\Delta pH$ -dependent gating (but see Villalba-Galea, 2014) postulated titratable sites that were alternatively accessible to external or internal solutions (Cherny et al., 1995). A systematic attempt to identify which site(s) was (were) involved revealed no single ionizable residue whose mutation to a non-ionizable residue abolished this phenomenon (Ramsey et al., 2010). Rather than protonation of a site, interaction of protonated water with the Arg residues in the S4 helix was suggested to effect  $\Delta pH$ -dependent gating (Ramsey et al., 2010). The possibility remained that multiple titratable sites are involved, an appealing idea because of the wide pH range over which the  $g_{H-V}$  relationship shifts according to the 40-mV rule. If one or more titratable sites are involved, the effect of pH might be expected to saturate. We demonstrate here that saturation of  $\Delta pH$ -dependent gating does occur above pH 8.0 in WT  $hH_V1$  (Fig. 3), consistent with previous observations in native rat proton currents (Cherny et al., 1995). Correspondingly, the regulatory sites proposed in our model were assigned a  $pK_a$  of 8.5, which was assumed to be same for access from internal or external solutions (Cherny et al., 1995).

Although distinct  $\Delta pH$ -dependent gating persists in  $hH_V1$  Trp<sup>207</sup> mutants, the pH at which saturation occurred dropped to  $pH_o$  7 but did not change for  $pH_i$ .

Evidently, mutation of Trp<sup>207</sup> lowers the apparent  $pK_a$  of the putative external site(s) without changing internal pH sensing. Despite not being titratable itself, Trp is evidently a key component in this mechanism, and may regulate the accessibility of another pH-sensing site, evidently increasing its effective  $pK_a$ . Because the same kind of  $pK_a$  shift occurs in both  $kH_V1$  and  $hH_V1$ , the putative titratable group(s) may be conserved in these species. In the closed  $mH_V1$  crystal structure (Takeshita et al., 2014) Arg<sup>207</sup> (R3) is twisted away from the pore into a hydrophobic pocket of the protein. If R3 is directed away from the aqueous pore, its  $pK_a$  may be decreased substantially (Kim et al., 2005) and could thus be a candidate pH regulatory site. However, mutation of R3 did not eliminate  $\Delta pH$ -dependent gating (Ramsey et al., 2010). Furthermore, experimental evidence indicates that Arg remains charged even inside proteins (Harms et al., 2011). Rather than viewing these effects as a change in effective  $pK_a$ , it is equally possible that mutation might alter the accessibility to protons of a site buried within the membrane electric field, by changing the effective dielectric constant in the pathway or the voltage drop to reach the site.

The results of this study indicate that both external and internal pH sensing may be accomplished by titratable groups with similar effective  $pK_a$  in WT  $hH_V1$  and in two unicellular marine species:  $kH_V1$  and  $EhH_V1$ . Furthermore, because the Trp<sup>207</sup> mutation in  $hH_V1$  (or the Trp<sup>176</sup> mutation in  $kH_V1$ ) selectively lowered the apparent  $pK_a$  for external but not internal pH, there appear to be distinct internal and external pH-sensing sites. This result speaks against the idea that a single site might alternatively sense  $pH_o$  and  $pH_i$  (Cherny et al., 1995), and indicates that distinct internal and external sensors (that must nevertheless interact with each other) are involved.

The kinetics of ion channel gating is often critical to their specialized function. The activation kinetics of voltage-gated  $Na^+$  and  $K^+$  channels is tunable by specific residues in S2 and S4 transmembrane segments (Lacroix et al., 2013). Here, we show that the highly conserved tryptophan residue in the S4 signature sequence of  $H_V1$  (RxWRxxR) is responsible for the characteristically slow kinetics of  $hH_V1$ . By stabilizing the closed state and optimizing  $\Delta pH$  sensing, Trp fine-tunes the threshold for channel opening, which in most species is just positive to  $E_H$ . Trp thus acts as a mechanism for adjusting the  $\Delta pH$ -dependent gating that is prerequisite to the functions of  $H_V1$  in all species.

We appreciate the generous gift of the  $EhH_V1$  construct by Alison Taylor (University of North Carolina, Chapel Hill, NC) and Colin Brownlee and Glen Wheeler (Marine Biological Association of the UK, The Laboratory, Plymouth, UK). The authors appreciate helpful discussions with Artem Ayuyan (Rush University, Chicago, IL) and Valerij Sokolov (Frumkin Institute of Physical Chemistry and Electrochemistry of the Russian Academy of Sciences, Moscow, Russia).



This work is supported by US National Science Foundation award MCB-0943362 and US National Institutes of Health (NIH) grant GM102336 (to T.E. DeCoursey and S.M.E. Smith). The content is solely the responsibility of the authors and does not necessarily represent the official views of the NIH.

The authors declare no competing financial interests.

Merritt C. Maduke served as editor.

Submitted: 11 June 2015

Accepted: 18 September 2015

**Note added in proof.** A recent EPR spectroscopy study of hHv1 (Li et al. 2015. The resting state of the human proton channel dimer in a lipid bilayer. *Proc. Natl. Acad. Sci. USA*. In press) showed that the dimer interface includes the top of S1 and the lower part of S4.

## REFERENCES

- Burley, S.K., and G.A. Petsko. 1986. Amino-aromatic interactions in proteins. *FEBS Lett.* 203:139–143. [http://dx.doi.org/10.1016/0014-5793\(86\)80730-X](http://dx.doi.org/10.1016/0014-5793(86)80730-X)
- Capasso, M., M.K. Bhamrah, T. Henley, R.S. Boyd, C. Langlais, K. Cain, D. Dinsdale, K. Pulford, M. Khan, B. Musset, et al. 2010. HVCN1 modulates BCR signal strength via regulation of BCR-dependent generation of reactive oxygen species. *Nat. Immunol.* 11:265–272. <http://dx.doi.org/10.1038/ni.1843>
- Chamberlin, A., F. Qiu, S. Rebolledo, Y. Wang, S.Y. Noskov, and H.P. Larsson. 2014. Hydrophobic plug functions as a gate in voltage-gated proton channels. *Proc. Natl. Acad. Sci. USA.* 111:E273–E282. <http://dx.doi.org/10.1073/pnas.1318018111>
- Cherny, V.V., V.S. Markin, and T.E. DeCoursey. 1995. The voltage-activated hydrogen ion conductance in rat alveolar epithelial cells is determined by the pH gradient. *J. Gen. Physiol.* 105:861–896. <http://dx.doi.org/10.1085/jgp.105.6.861>
- Chester, R., and T.D. Jickells. 2012. Marine Geochemistry. Vol. Third edition. Wiley-Blackwell, Hoboken, NJ. 420 pp. <http://dx.doi.org/10.1002/9781118349083>
- DeCoursey, T.E. 2003. Voltage-gated proton channels and other proton transfer pathways. *Physiol. Rev.* 83:475–579. <http://dx.doi.org/10.1152/physrev.00028.2002>
- DeCoursey, T.E. 2010. Voltage-gated proton channels find their dream job managing the respiratory burst in phagocytes. *Physiology (Bethesda)*. 25:27–40. <http://dx.doi.org/10.1152/physiol.00039.2009>
- DeCoursey, T.E. 2013. Voltage-gated proton channels: molecular biology, physiology, and pathophysiology of the Hv family. *Physiol. Rev.* 93:599–652. <http://dx.doi.org/10.1152/physrev.00011.2012>
- DeCoursey, T.E., and V.V. Cherny. 1997. Deuterium isotope effects on permeation and gating of proton channels in rat alveolar epithelium. *J. Gen. Physiol.* 109:415–434. <http://dx.doi.org/10.1085/jgp.109.4.415>
- DeCoursey, T.E., and V.V. Cherny. 1998. Temperature dependence of voltage-gated H<sup>+</sup> currents in human neutrophils, rat alveolar epithelial cells, and mammalian phagocytes. *J. Gen. Physiol.* 112:503–522. <http://dx.doi.org/10.1085/jgp.112.4.503>
- DeCoursey, T.E., and E. Ligeti. 2005. Regulation and termination of NADPH oxidase activity. *Cell. Mol. Life Sci.* 62:2173–2193. <http://dx.doi.org/10.1007/s00018-005-5177-1>
- DeCoursey, T.E., D. Morgan, and V.V. Cherny. 2003. The voltage dependence of NADPH oxidase reveals why phagocytes need proton channels. *Nature.* 422:531–534. <http://dx.doi.org/10.1038/nature01523>
- Dudev, T., B. Musset, D. Morgan, V.V. Cherny, S.M.E. Smith, K. Mazmanian, T.E. DeCoursey, and C. Lim. 2015. Selectivity mechanism of the voltage-gated proton channel, Hv1. *Sci Rep.* 5:10320. <http://dx.doi.org/10.1038/srep10320>
- Fischer, H. 2012. Function of proton channels in lung epithelia. *Wiley Interdiscip Rev Membr Transp Signal.* 1:247–258. <http://dx.doi.org/10.1002/wmts.17>
- Fogel, M., and J.W. Hastings. 1972. Bioluminescence: mechanism and mode of control of scintillon activity. *Proc. Natl. Acad. Sci. USA.* 69:690–693. <http://dx.doi.org/10.1073/pnas.69.3.690>
- Fujiwara, Y., T. Kurokawa, K. Takeshita, M. Kobayashi, Y. Okochi, A. Nakagawa, and Y. Okamura. 2012. The cytoplasmic coiled-coil mediates cooperative gating temperature sensitivity in the voltage-gated H<sup>+</sup> channel Hv1. *Nat. Commun.* 3:816. <http://dx.doi.org/10.1038/ncomms1823>
- Gallivan, J.P., and D.A. Dougherty. 1999. Cation- $\pi$  interactions in structural biology. *Proc. Natl. Acad. Sci. USA.* 96:9459–9464. <http://dx.doi.org/10.1073/pnas.96.17.9459>
- Harms, M.J., J.L. Schlessman, G.R. Sue, and B. García-Moreno. 2011. Arginine residues at internal positions in a protein are always charged. *Proc. Natl. Acad. Sci. USA.* 108:18954–18959. <http://dx.doi.org/10.1073/pnas.1104808108>
- Henderson, L.M., J.B. Chappell, and O.T.G. Jones. 1987. The superoxide-generating NADPH oxidase of human neutrophils is electrogenic and associated with an H<sup>+</sup> channel. *Biochem. J.* 246:325–329. <http://dx.doi.org/10.1042/bj2460325>
- Hondares, E., M.A. Brown, B. Musset, D. Morgan, V.V. Cherny, C. Taubert, M.K. Bhamrah, D. Coe, F. Marelli-Berg, J.G. Gribben, et al. 2014. Enhanced activation of an amino-terminally truncated isoform of the voltage-gated proton channel HVCN1 enriched in malignant B cells. *Proc. Natl. Acad. Sci. USA.* 111:18078–18083. <http://dx.doi.org/10.1073/pnas.1411390111>
- Iovannisci, D., B. Illek, and H. Fischer. 2010. Function of the HVCN1 proton channel in airway epithelia and a naturally occurring mutation, M91T. *J. Gen. Physiol.* 136:35–46. <http://dx.doi.org/10.1085/jgp.200910379>
- Killian, J.A., and G. von Heijne. 2000. How proteins adapt to a membrane-water interface. *Trends Biochem. Sci.* 25:429–434. [http://dx.doi.org/10.1016/S0968-0004\(00\)01626-1](http://dx.doi.org/10.1016/S0968-0004(00)01626-1)
- Kim, J., J. Mao, and M.R. Gunner. 2005. Are acidic and basic groups in buried proteins predicted to be ionized? *J. Mol. Biol.* 348:1283–1298. <http://dx.doi.org/10.1016/j.jmb.2005.03.051>
- Koch, H.P., T. Kurokawa, Y. Okochi, M. Sasaki, Y. Okamura, and H.P. Larsson. 2008. Multimeric nature of voltage-gated proton channels. *Proc. Natl. Acad. Sci. USA.* 105:9111–9116. <http://dx.doi.org/10.1073/pnas.0801553105>
- Kulleperuma, K., S.M.E. Smith, D. Morgan, B. Musset, J. Holyoake, N. Chakrabarti, V.V. Cherny, T.E. DeCoursey, and R. Pomès. 2013. Construction and validation of a homology model of the human voltage-gated proton channel hHv1. *J. Gen. Physiol.* 141:445–465.
- Kuno, M., H. Ando, H. Morihata, H. Sakai, H. Mori, M. Sawada, and S. Oiki. 2009. Temperature dependence of proton permeation through a voltage-gated proton channel. *J. Gen. Physiol.* 134:191–205. <http://dx.doi.org/10.1085/jgp.200910213>
- Lacroix, J.J., F.V. Campos, L. Frezza, and F. Bezanilla. 2013. Molecular bases for the asynchronous activation of sodium and potassium channels required for nerve impulse generation. *Neuron.* 79:651–657. <http://dx.doi.org/10.1016/j.neuron.2013.05.036>
- Lee, S.Y., J.A. Letts, and R. Mackinnon. 2008. Dimeric subunit stoichiometry of the human voltage-dependent proton channel Hv1. *Proc. Natl. Acad. Sci. USA.* 105:7692–7695. <http://dx.doi.org/10.1073/pnas.0803277105>
- Li, Q., S. Wanderling, M. Paduch, D. Medovoy, A. Singharoy, R. McGreevy, C.A. Villalba-Galea, R.E. Hulse, B. Roux, K. Schulten, et al. 2014. Structural mechanism of voltage-dependent gating in an isolated voltage-sensing domain. *Nat. Struct. Mol. Biol.* 21:244–252. <http://dx.doi.org/10.1038/nsmb.2768>
- Lishko, P.V., I.L. Botchkina, A. Fedorenko, and Y. Kirichok. 2010. Acid extrusion from human spermatozoa is mediated by flagellar

- voltage-gated proton channel. *Cell*. 140:327–337. <http://dx.doi.org/10.1016/j.cell.2009.12.053>
- MacCallum, J.L., W.F.D. Bennett, and D.P. Tieleman. 2008. Distribution of amino acids in a lipid bilayer from computer simulations. *Biophys. J.* 94:3393–3404. <http://dx.doi.org/10.1529/biophysj.107.112805>
- Morgan, D., and T.E. DeCoursey. 2014. Analysis of electrophysiological properties and responses of neutrophils. *Methods Mol. Biol.* 1124:121–158. [http://dx.doi.org/10.1007/978-1-62703-845-4\\_9](http://dx.doi.org/10.1007/978-1-62703-845-4_9)
- Morgan, D., M. Capasso, B. Musset, V.V. Cherny, E. Ríos, M.J.S. Dyer, and T.E. DeCoursey. 2009. Voltage-gated proton channels maintain pH in human neutrophils during phagocytosis. *Proc. Natl. Acad. Sci. USA*. 106:18022–18027. <http://dx.doi.org/10.1073/pnas.0905565106>
- Morgan, D., B. Musset, K. Kulleperuma, S.M.E. Smith, S. Rajan, V.V. Cherny, R. Pomès, and T.E. DeCoursey. 2013. Peregrination of the selectivity filter delineates the pore of the human voltage-gated proton channel hHv1. *J. Gen. Physiol.* 142:625–640. <http://dx.doi.org/10.1085/jgp.201311045>
- Musset, B., V.V. Cherny, D. Morgan, Y. Okamura, I.S. Ramsey, D.E. Clapham, and T.E. DeCoursey. 2008a. Detailed comparison of expressed and native voltage-gated proton channel currents. *J. Physiol.* 586:2477–2486. <http://dx.doi.org/10.1113/jphysiol.2007.149427>
- Musset, B., D. Morgan, V.V. Cherny, D.W. MacGlashan Jr., L.L. Thomas, E. Ríos, and T.E. DeCoursey. 2008b. A pH-stabilizing role of voltage-gated proton channels in IgE-mediated activation of human basophils. *Proc. Natl. Acad. Sci. USA*. 105:11020–11025. <http://dx.doi.org/10.1073/pnas.0800886105>
- Musset, B., S.M.E. Smith, S. Rajan, V.V. Cherny, D. Morgan, and T.E. DeCoursey. 2010. Oligomerization of the voltage-gated proton channel. *Channels (Austin)*. 4:260–265. <http://dx.doi.org/10.4161/chan.4.4.12789>
- Musset, B., S.M.E. Smith, S. Rajan, D. Morgan, V.V. Cherny, and T.E. DeCoursey. 2011. Aspartate 112 is the selectivity filter of the human voltage-gated proton channel. *Nature*. 480:273–277. <http://dx.doi.org/10.1038/nature10557>
- Musset, B., R.A. Clark, T.E. DeCoursey, G.L. Petheo, M. Geiszt, Y. Chen, J.E. Cornell, C.A. Eddy, R.G. Brzyski, and A. ElJamali. 2012. NOX5 in human spermatozoa: expression, function, and regulation. *J. Biol. Chem.* 287:9376–9388. <http://dx.doi.org/10.1074/jbc.M111.314955>
- Papazian, D.M., X.M. Shao, S.A. Seoh, A.F. Mock, Y. Huang, and D.H. Wainstock. 1995. Electrostatic interactions of S4 voltage sensor in Shaker K<sup>+</sup> channel. *Neuron*. 14:1293–1301. [http://dx.doi.org/10.1016/0896-6273\(95\)90276-7](http://dx.doi.org/10.1016/0896-6273(95)90276-7)
- Pettersen, E.F., T.D. Goddard, C.C. Huang, G.S. Couch, D.M. Greenblatt, E.C. Meng, and T.E. Ferrin. 2004. UCSF Chimera—a visualization system for exploratory research and analysis. *J. Comput. Chem.* 25:1605–1612. <http://dx.doi.org/10.1002/jcc.20084>
- Ramsey, I.S., M.M. Moran, J.A. Chong, and D.E. Clapham. 2006. A voltage-gated proton-selective channel lacking the pore domain. *Nature*. 440:1213–1216. <http://dx.doi.org/10.1038/nature04700>
- Ramsey, I.S., Y. Mokrab, I. Carvacho, Z.A. Sands, M.S.P. Sansom, and D.E. Clapham. 2010. An aqueous H<sup>+</sup> permeation pathway in the voltage-gated proton channel Hv1. *Nat. Struct. Mol. Biol.* 17:869–875. <http://dx.doi.org/10.1038/nsmb.1826>
- Roos, A., and W.F. Boron. 1981. Intracellular pH. *Physiol. Rev.* 61:296–434.
- Santiveri, C.M., and M.A. Jiménez. 2010. Tryptophan residues: scarce in proteins but strong stabilizers of  $\beta$ -hairpin peptides. *Biopolymers*. 94:779–790. <http://dx.doi.org/10.1002/bip.21436>
- Smith, S.M.E., D. Morgan, B. Musset, V.V. Cherny, A.R. Place, J.W. Hastings, and T.E. DeCoursey. 2011. Voltage-gated proton channel in a dinoflagellate. *Proc. Natl. Acad. Sci. USA*. 108:18162–18167. <http://dx.doi.org/10.1073/pnas.1115405108>
- Takeshita, K., S. Sakata, E. Yamashita, Y. Fujiwara, A. Kawanabe, T. Kurokawa, Y. Okochi, M. Matsuda, H. Narita, Y. Okamura, and A. Nakagawa. 2014. X-ray crystal structure of voltage-gated proton channel. *Nat. Struct. Mol. Biol.* 21:352–357. <http://dx.doi.org/10.1038/nsmb.2783>
- Tatko, C.D., and M.L. Waters. 2003. The geometry and efficacy of cation- $\pi$  interactions in a diagonal position of a designed  $\beta$ -hairpin. *Protein Sci.* 12:2443–2452. <http://dx.doi.org/10.1110/ps.03284003>
- Taylor, A.R., A. Chrachri, G. Wheeler, H. Goddard, and C. Brownlee. 2011. A voltage-gated H<sup>+</sup> channel underlying pH homeostasis in calcifying coccolithophores. *PLoS Biol.* 9:e1001085. <http://dx.doi.org/10.1371/journal.pbio.1001085>
- Tombola, F., M.H. Ulbrich, and E.Y. Isacoff. 2008. The voltage-gated proton channel Hv1 has two pores, each controlled by one voltage sensor. *Neuron*. 58:546–556. <http://dx.doi.org/10.1016/j.neuron.2008.03.026>
- Villalba-Galea, C.A. 2014. Hv1 proton channel opening is preceded by a voltage-independent transition. *Biophys. J.* 107:1564–1572. <http://dx.doi.org/10.1016/j.bpj.2014.08.017>
- Wang, Y., S.J. Li, X. Wu, Y. Che, and Q. Li. 2012. Clinicopathological and biological significance of human voltage-gated proton channel Hv1 protein overexpression in breast cancer. *J. Biol. Chem.* 287:13877–13888. <http://dx.doi.org/10.1074/jbc.M112.345280>
- Wood, M.L., E.V. Schow, J.A. Freitas, S.H. White, F. Tombola, and D.J. Tobias. 2012. Water wires in atomistic models of the Hv1 proton channel. *Biochim. Biophys. Acta*. 1818:286–293. <http://dx.doi.org/10.1016/j.bbame.2011.07.045>
- Wu, L.J., G. Wu, M.R. Akhavan Sharif, A. Baker, Y. Jia, F.H. Fahey, H.R. Luo, E.P. Feener, and D.E. Clapham. 2012. The voltage-gated proton channel Hv1 enhances brain damage from ischemic stroke. *Nat. Neurosci.* 15:565–573. <http://dx.doi.org/10.1038/nn.3059>